Smart Structures and Systems, *Vol. 27, No. 1 (2021) 19-33*
DOI: https://doi.org/10.12989/sss.2021.27.1.019

Implementation of SHM system for Hangzhou East Railway Station using a wireless sensor network

Yanbin Shen [1a], Wenwei Fu [1], Yaozhi Luo*[1], Chung-Bang Yun [1], Dun Liu [2], Pengcheng Yang [3], Guang Yang [4] and Guangen Zhou [5]

[1] *College of Civil Engineering and Architecture, Zhejiang University, Hangzhou 310058, China*
[2] *CITIC General Institute of Architectural Design and Research Co., Ltd, Wuhan 430014, China*
[3] *Country Garden Holdings Company Limited, Hong Kong 999077, China*
[4] *China Railway SIYUAN Survey & Design Group Co., Ltd, Wuhan 430063, China*
[5] *Zhejiang Southeast Space Frame Company, Hangzhou 311209, China*

(*Received August 7, 2019, Revised October 31, 2020, Accepted November 5, 2020*)

Abstract. Structural health monitoring (SHM) is facilitated by new technologies that involve wireless sensor networks (WSNs). The main benefits of WSNs are that they are distributed, are inexpensive to install, and manage data effectively via remote control. In this paper, a wireless SHM system for the steel structure of Hangzhou East Railway Station in China is developed, since the state of the structural life cycle is highly complicated and the accompanying internal force redistribution is not known. The monitoring system uses multitype sensors, which include stress, acceleration, wind load, and temperature sensors, as the measurement components for the structural features, construction procedure, and on-site environment. The sensor nodes communicate with each other via a flexible tree-type network. The system that consists of 323 sensors is designed for the structure, and the data acquisition process will continue throughout its whole life cycle. First, a full-scale application of SHM using a WSN is described in details. Then, it focuses on engineering practice and data analysis. The current customized WSN has been demonstrated to have satisfactory durability and strong robustness; hence, it well satisfies the requirements for multi-type sensors to operate in a large area. The data analysis results demonstrate that the effects of the construction process and the environment on the super-large-scale structure have been captured accurately. Those effects include the stress variation throughout the construction process, the dynamic responses that are caused by passing trains, the strain variation caused by temperature change over the long term, and the delay in the wind-pressure history.

Keywords: wireless sensor network; life-cycle; structural health monitoring; railway station

1. Introduction

Increasingly more civil infrastructures such as skyscrapers, long-span bridges, and offshore structures are monitored by structural health monitoring (SHM) systems to evaluate their life cycle performance. Therefore, increasing attention is being paid to studies on SHM, for which a wired or wireless sensor network (WSN) is utilized. The disadvantages of traditional wired sensor networks are that they are difficult and expensive to install and are easily damaged during construction. Consequently, the application of a WSN is a better choice since it can offer an economical, easy to install, and flexible solution to long-distance, and scalable SHM for large-scale civil infrastructures. Wireless sensing technology was first applied in an SHM system for civil engineering (Straser and Kiremidjian 1996, Straser *et al*. 2001). Thereafter, many studies were conducted on the development of various types of wireless sensors, and many research prototypes of WSNs were proposed. One remarkable achievement is the design of a wireless sensor node that utilizes an 8-bit microchip and uses an accelerometer as the sensor component. It has been verified in the lab and has laid a foundation for future applications in engineering (Lynch *et al*. 2001). The development of wireless sensor technology has kept up with the current age and has become more advanced.

In recent years, wireless sensor nodes for applications such as vibration sensing (Ruiz-Sandoval *et al*. 2003, Jang *et al*. 2010, Park *et al*. 2010, Dong *et al*. 2014), strain sensing (Lee *et al*. 2010), displacement sensing (Hou *et al*. 2005, Zonta *et al*. 2010), and environmental sensing (Jo *et al*. 2011) have been presented by researchers. In the case of health monitoring of bridge structures, wireless acceleration sensors are very important and widely applied. For large-span spatial structures, the stress distribution, which is obtained by comparing the design strengths of structural members, is important for safety assessment; hence, wireless strain-type sensors are installed to directly measure the strain of components (Luo *et al*. 2014, Zhang and Luo 2017). Among the variety of strain sensors, a wireless vibrating wire sensor (VWS) node that was developed by Korean researchers stands out (Lee *et al*. 2010). It can be applied to long-term stress monitoring due to its stability and durability (Park *et al*. 2013). For a super-large-scale

*Corresponding author, Professor,
E-mail: luoyz@zju.edu.cn
[a] Associate Professor, E-mail: ybshen@zju.edu.cn

ISSN: 1738-1584 (Print), 1738-1991 (Online)

structure, multiple types and a large number of sensors shall be installed, and the optimal sensor placement must be considered (Yi *et al*. 2015). Structures are always subjected to various adverse factors during their long service lives; thus, real-time data are of substantial value for implementing an effective maintenance strategy (Yi *et al*. 2018).

The real-world application of WSN technology in civil engineering tends to fall behind the research work, and many researchers have employed WSNs that have more customized functions to monitor structures. (Kim *et al*. 2007, He *et al*. 2018). A relatively early application in 1997 that has been reported worldwide was monitoring the environment and behavior of a bridge (Maser *et al*. 1996). Since then, the speed of development of this technology in the field of bridge health monitoring using WSNs has been increasing (Meyer *et al*. 2010, Spencer and Cho 2011). A benchmark SHM system for tall buildings was installed on the 600-m-high Canton Tower in Guangzhou, which integrated many and various types of wired sensors with a small amount of sensor technology (Ni *et al*. 2009, 2011). SHM systems have also been applied at Shenzhen Civilization Centre, Chinese National Aquatics Centre, and FAST (Five-hundred-meter Aperture Spherical radio Telescope). However, only a small number of wireless sensors were used to monitor those buildings, and optical fiber sensors are still the main monitoring instruments (Teng *et al*. 2010, Qu *et al*. 2006, Sun *et al*. 2015). The full-scale application of SHM on spatial structures remains rare to this day. Sensors deployed on structures are commonly single, and the data transfer mechanism between sensor nodes is not deployable and flexible. WSNs such as this will limit the installation of sensors during the construction stage, which will cause the monitoring data to not be recorded in this stage. Meanwhile, the long-term the performance of the monitoring system of spatial structures during its life-cycle deserves to be evaluated carefully.

This paper presents a customized WSN that was developed for monitoring structural components that may affect the safety, serviceability, and durability of the Hangzhou East Railway Station throughout its life-cycle. A full-scale SHM system with various sensors for stress, acceleration, wind load, and temperature as the measurement components has been implemented. The sensor nodes communicate with each other by using a flexible tree-type network, and the collected data are transferred from the sensor nodes to the cloud server. This paper focuses on the full-scale deployment of an SHM using a customized WSN and it addresses the following issues: (1) research work on the design and setup of the SHM system; (2) the full-scale application of SHM and (3) the working performance of the SHM system, including a brief discussion on the monitoring data during the construction and in-service stages. With the full-scale application of this SHM system, the amount of available monitoring data has increased substantially, and the level of understanding regarding the structural characteristics is significantly boosted.

2. Design and setup of the SHM system

To investigate the structural features of large-span spatial structures and on-site environments, it is essential to develop a customized monitoring system for structural and environmental parameter monitoring, that can satisfy the requirement of the full-scale deployment on the structure. There are three crucial features concerning the full-scale deployment, namely the design of the wireless sensor nodes, the topology of the WSN, and the remote operation system.

2.1 Design of the wireless sensor nodes

The wireless sensor node is the basic component of the wireless monitoring system. The hardware for a sensor node typically consists of four parts that perform the following functions: data acquisition, digital wireless communication, embedded micro-processing, and power management (Straser and Kiremidjian 1996, Lynch *et al*. 2001). Various principles are commonly considered in the hardware design of wireless sensor nodes, such as functional modularity, measurement accuracy, configuration flexibility, network extensibility, and energy efficiency. Several modules are designed to realize the functions specified above: the power management (PM), micro control unit (MCU), radio frequency (RF), static random-access memory (SRAM), and multitype sensing (MTS) modules.

The newly developed MTS module contains various sensors, analog-to-digital converters, and amplifier circuits, which enable the sampling of various parameters. Via the RF module, wireless network topologies and protocols can be implemented independently without interfering with other circuit units and configurations. The MCU is the core of the wireless sensor nodes. In addition to realize the above four functions, it also contains a clock module to solve the time-sync problem. The clock module consists of a low-power real-time clock chip, which can be used to set the exact time for data collection. By using an FM radio-based time synchronization scheme, the internal time of sensor nodes is calibrated. The PM module adopts a suitable energy management strategy, which is closely related to the monitoring scheme, to extend the operating time of the sensor nodes.

Fig. 1 illustrates the architecture of a wireless sensor node. The MTS module is installed on an individual board, while the other modules are integrated into another board. Fig. 2 shows the integrated wireless sensor unit using two printed circuit boards (PCBs). The MTS module can be divided into four sensing types for multiple sensors, as illustrated in Fig. 3. All sensors except VWS can produce a digital signal output that can be directly obtained without ADC. Only the VWS requires a specified analogue circuit for excitation and picking up the signal. For a different monitoring component, the corresponding sensor node is selected, which only controls a particular type of sensor unit with a specific sampling rate. The program on the MTS module can be rewritten for different types of sensor units. To implement the network control, a length of 64 bytes is often set for each communication packet, which includes

the ID numbers of the sensor node, the piconet number, and the command type, as illustrated in Fig. 4. Considering the requirements of all types of MTS modules for various sensors, the length of the data array is defined as 52 bytes.

2.2 Remote operating system

All data that are collected from multitype sensor nodes through the sink node can be subsequently transmitted to the authorized terminal via the internet, and all sensor nodes can receive action instructions. Thus, the whole framework of the remote operating system for sending the commands and transmitting the data of the monitoring system is designed accordingly as shown in Fig. 5. The first step is to put the system online. An on-site industrial PC (IPC) is commonly used to make the connection via a cable or wireless local area networks (WLANs). Through universal serial bus (USB) ports or the serial ports of the PC, the extension layer of the sink node can communicate with the IPC via serial protocols. A strong advantage of using an on-site IPC is that it can process the raw data easily. Any authorized terminal can exchange data with the on-site server. The processed data can be displayed and analysed in real time.

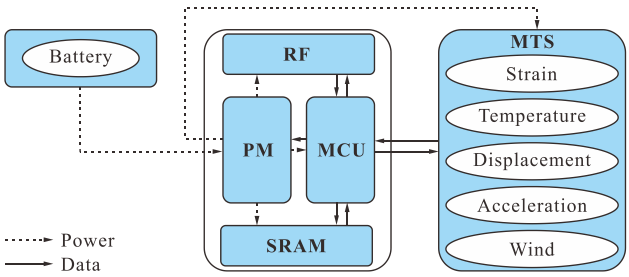

Fig. 1 Hardware architecture of a wireless sensor node

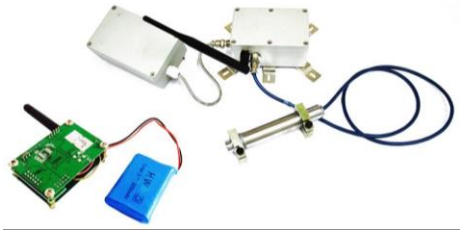

Fig. 2 Pictures of a wireless sensor unit

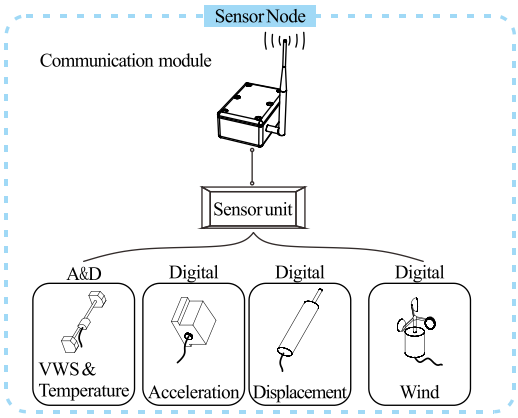

Fig. 3 Multi-type sensors for four types of measurements

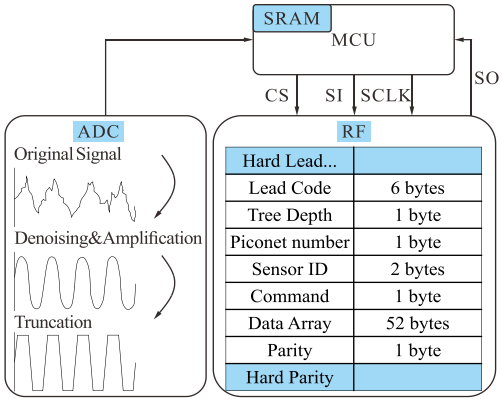

Fig. 4 Protocol and format of the signal in sensor nodes

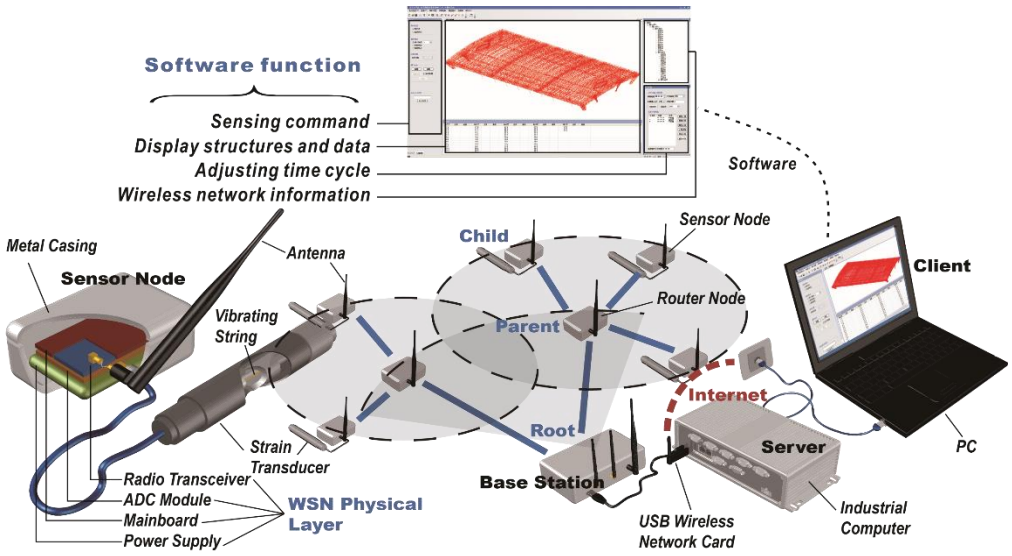

Fig. 5 The whole framework of the remote operating system

In the implementation of WSNs, researchers focus on power management strategies. On bridge structures, sensing nodes are typically exposed to sunlight; therefore, energy harvesting during the long-term monitoring period is realizable by installing solar panels (Rice *et al*. 2010). However, the sensor nodes deployed on spatial structures are often sheltered by the roof sheathing after construction has been completed. As a result, rechargeable batteries with a voltage of up to 3.7 V are selected as the power system of all nodes. To extend the working time of each battery charge, special work patterns, including sleeping mode and operating mode, are used on each sensor node. Each sensor node spends most of the time in sleeping mode and wakes up for a short moment at a specified time cycle (Ye *et al*. 2002). Researchers and engineering administrators can control those work patterns through the remote operating system. To unify the network control, the sampling frequency and time for individual sensors are regulated. Then, users can adjust the time cycle at any time as required. Using this approach, the regular battery replacement period is longer than 6 months. The functions of the WSN that were discussed earlier are performed with the support of specialized software that is installed on the IPC. In addition, displaying the structure and data, identifying the sink node, and storing and updating data to terminal devices via the internet are included as its main functions.

2.3 Topology of a WSN

When all sensors that have been scattered in the sensor field are ready, they collect data and route the data back to the sink node (Akyildiz *et al*. 2002). A sink node, several relay nodes (routing nodes), and many sensor nodes operate in synergy as a well-developed wireless sensor network. Due to the distance limit in wireless data transmission, the design of a suitable communication network for sensor nodes is necessary. According to the relationships among the nodes, the chain topology, star topology, mesh topology, and tree topology are defined (Townsend and Arms 2005). The network topology determines the power consumption and the lifespan of a WSN. A star-type topology in which a sink node sends commands to sensor nodes directly and exclusively is limited by the radio range. Although a WSN in a mesh topology has no transmission distance limit, it must balance the overall power consumption (De Battista 2013, Zou *et al*. 2014). A network with tree-type topology is similar to a tree with branches of all connected relay nodes and leaves of numerous sensor nodes. the relay nodes divide the whole tree-type network into many star-type piconets.

Table 1 Full-scale wireless SHM systems for civil infrastructure

Civil structure	Structure type	Structure size	Sensor types and total number	Network type	Main characteristic
Golden Gate Bridge (Pakzad *et al*. 2008)	Suspension bridge	Span of 1,965.8 m	(2) and, (3) Total number:64	Chain-type	Development of a WSN for identifying vibration modes
Jindo Bridge (Jang *et al*. 2010)	Cable-stayed bridge	Span of 484 m	(1-5) and, (8) Total number: 669	Chain-type	Deployment of a WSN for full-scale, continuous, autonomous SHM
Yongjong Grand Bridge (Chae *et al*. 2011)	Suspension bridge	Span of 550 m	(1-3) and, (5) Total number: 45	Mesh/Star-type	Development of a prototype of a wireless-sensor based SHM system
Bobby Dodd Stadium (Phanish *et al*. 2015)	Truss structure	Not provided	(3) Total number: 45	Star-type	Development of a WSN with high time synchronization and accuracy
Hangzhou Olympic Center Stadium (Zhang and Luo 2017)	Pipe-truss structure	Area of 74,500 m^2	(1-2) and, (7) Total number: 823	Tree-type	Application of a wireless SHM system to grasp the evolution of the structure's performance
Revolving auditorium (Luo *et al*. 2014)	Truss structure	Area of 1,705 m^2	(1) and, (2) Total number:52	Ring-type	Realization of monitoring a moving structure by using a WSN
Prague Metro (Bennett *et al*. 2010)	Tunnel structure	Length of 350 m	(8) and, (9) Total number:21	Chain-type	Installation of a WSN in an underground environment
London tunnel (Stajano *et al*. 2010)	Tunnel structure	Length of 180 m	(2), (4) and, (10) Total number: 13	Chain-type	Development of a prototype wireless SHM system in an underground environment
Torre Aquila (Zonta *et al*. 2010)	Medieval tower	Height of 31 m	(2), (3-4) and, (10) Total number: 16	Tree-type	Using a WSN for heritage site assessment
Vestas turbine (Swartz *et al*. 2010)	Wind turbine	Height of 76.1 m	(1) and, (3) Total number:10	Chain-type	Application of a wireless SHM system under electromagnetic interference
Hangzhou East Railway Station	Pipe-truss structure	Area of 146,563 m^2	(1-3), (5) and, (6) Total number: 306	Tree-type	Full-scale application of a WSN in a large-area steel structure

*Note: (1) strain gauges; (2) temperature sensors; (3) accelerometers; (4) displacement transducers; (5) anemographs; (6) wind pressure sensors; (7) total stations; (8) inclinometers; (9) crack sensors; (10) humidity sensors

In each piconet, the central relay node is a commander that is in charge of all sensor nodes. The piconet can be reorganized via address reassignment: If the connection between a sensor node and a relay node is weak while the connection between the same sensor node and another relay node is strong, a new route will be redefined by reassigning new addresses to the relay node that has a stronger connection. Therefore, robust communication over the entire network can be realized. A sink node is the core part of the entire tree-type network and constitutes a base station along with an on-site server.

Many civil structures all over the world have SHM systems using WSNs installed. The features of some civil structures, which include the structure types, structure size, sensor types, sensor numbers, network type and main characteristics of the wireless SHM system, that are implemented with WSNs are summarized in Table 1. It has found that the chain-type network is commonly used in slender structures, such as bridges, tunnels, etc. For a circular building, a special chain-type network, a ring-type network, can be used for network topology design. To enlarge the network coverage area, the tree-type network is designed for large-area structures such as stadiums and railway stations. It is important to set up rational network topologies to shorten wireless transmission distance and increase the energy efficiency of SHM systems. Based on a comprehensive analysis of multiple factors, the tree-type network was adopted for Hangzhou East Railway Station.

In a network with a tree-type topology, the node address is defined by several numbers. In a three-layer tree-type network, three-number addresses are used for applications. The first number stands for the branch of the tree-type network, the second number indicates the relay node of the piconet, and the third number represents the sensor node. For example, the ID address for the 14th sensor node in the piconet of the second relay node within the second branch will be 2.2.14. The encoded form of the ID address on each layer is presented in Fig. 6. To improve the communication efficiency and stability, each node is assigned a specified ID address. Each node only saves a subset of the ID addresses and uses them to communicate with relevant nodes. For example, a relay node only saves the ID addresses of its superior relay node and its subordinate node, and a sensor node saves the ID address of its parent node, namely, the relay node of the same piconet.

There are two methods of communication between relay nodes and sensor nodes: broadcast and unicast. In broadcast, all nodes within the signal area are woken up and can decide whether to execute or not. Thus, broadcast is used to wake up sensor nodes and to command them to start sampling. In contrast, the commands in unicast include a destination address and are to be executed only by the specified node. Thus, unicast is used for all other commands, such as data call-back and address reassignment.

3. Full-scale application of an SHM

Similar wireless SHM systems as described above, have been applied in several real-world cases (Luo *et al*. 2014). In this paper for the Hangzhou East Railway Station, the new challenges of the work for the customized SHM system mainly include the following aspects: the application of the WSN for a super-large area over 10,000 m^2, good performance for multiple parameter sampling over a long term, an expandable network topology design adapting to the accumulative structure forming, and high time synchronization accuracy over the long term.

3.1 Railway station description

The Hangzhou East Railway Station is one of the nine super-large-scale railway stations in China and can accommodate 120,000 passengers a day, as shown in Fig. 7.

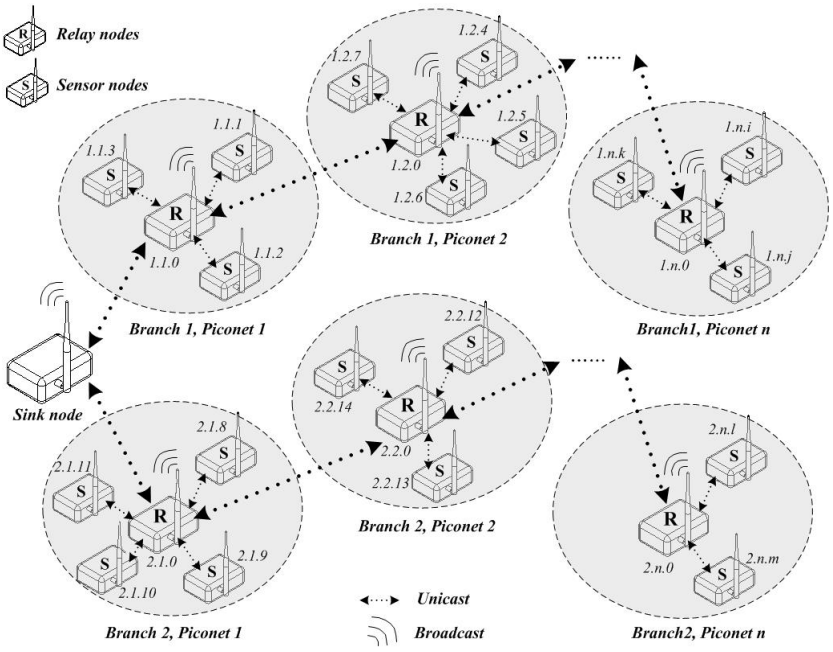

Fig. 6 Topology of the tree-type network and ID addresses

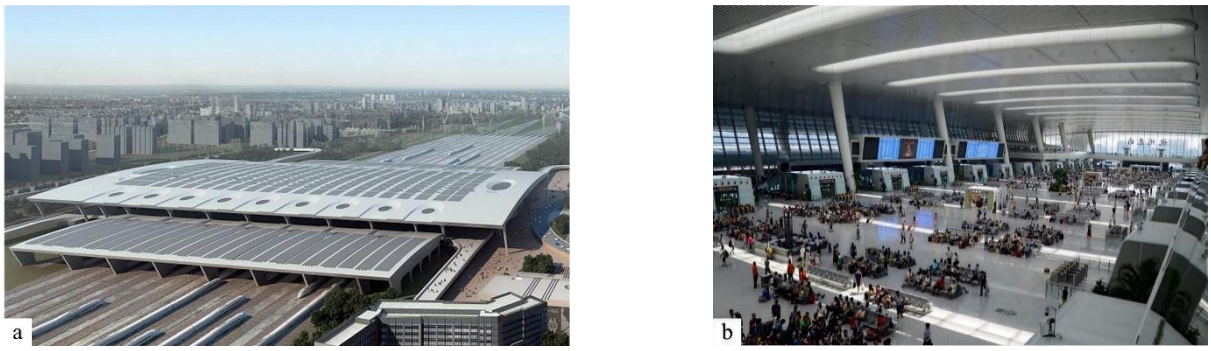

(a) Structure of the railway station (b) Inside view of the station

Fig. 7 Photographs of the Hangzhou East Railway Station

An aerial view shows that the building is rectangular with a length of 514.8 meters in the east-west direction and a width of 284.7 meters. The entire steel structure of the station can be divided into three parts, as illustrated in Fig. 8: a cross-connection pipe-truss roof with a maximum span of 111 meters (the middle part along the south-north direction), fifty-four large variable ellipse-shaped cross-section columns with a maximum diameter of 5.79 m, and eight large latticed columns (at the east and west ends).

The monitoring work of Hangzhou East Railway Station has been divided into two stages: the construction stage and the in-service stage. During the construction stage, the construction process integrates several construction technologies, such as integral truss lifting, scaffold installation, and block hoisting. To monitor the construction process of the real structure, the installation of the WSN was launched from both the east and west sides, and the network was connected in the middle. Because the internal force redistribution during the construction procedures is very complicated, the internal forces of the structure may differ from the values of the initial design. In the in-service stage, the structure is subjected to not only the environmental loadings but also to the vibration that is caused by the movements of the trains. To track the structural condition throughout the life cycle, which includes the construction stage and in-service stage, the monitoring system is deployed at the beginning of the construction stage. The monitored structural components mainly include the pipe trusses, ellipse-shape columns, and large latticed columns. Another feature of a super-large-scale railway station of this type is the "bridge-building combination", namely, trains must pass through the station; hence, the vibration that is caused by the trains cannot be ignored. Considering all the factors that may affect the structure, various types of sensors, such as vibrating wire sensors for strains, temperature sensors, acceleration sensors, wind pressure sensors, and anemographs, are included in the monitoring system.

3.2 Implementation of a WSN

After a series of performance tests in the lab, the customized WSN was installed on Hangzhou East Railway Station. The application is discussed below. There are two or four VWSs installed on the surfaces of the pipes and columns in each section, namely, two on truss pipes and four on columns, which record the axial force and the bending moment. In Eq. (1), ε_1 and ε_2 represent two symmetrical surface strains. For a clearer comparison, S_A and S_B are defined as the axial and bending stresses, respectively, in Eq. (2)

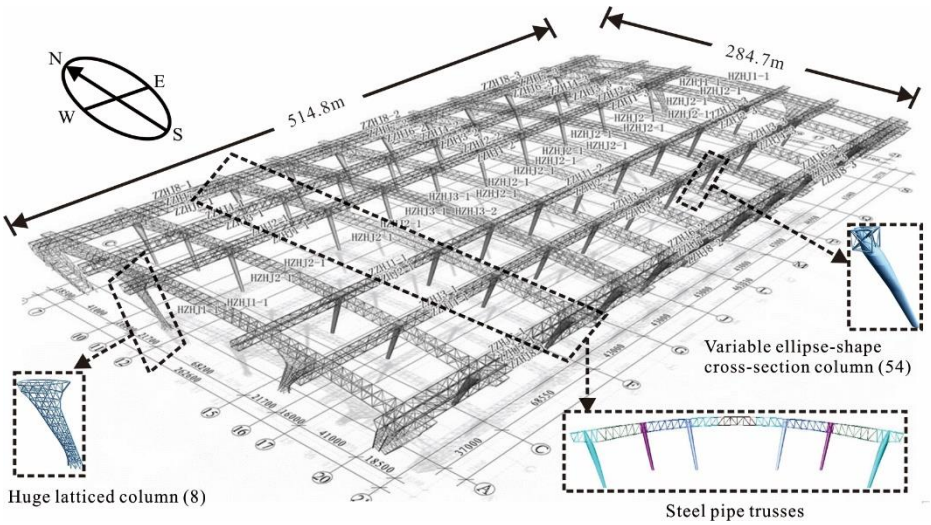

Fig. 8 Structural view of the Hangzhou East Railway Station

$$\begin{cases} N = EA\dfrac{\varepsilon_1 + \varepsilon_2}{2} \\ M = \dfrac{EI}{R}\dfrac{\varepsilon_1 - \varepsilon_2}{2} \end{cases} \quad (1)$$

$$\begin{cases} S_A = E\dfrac{\varepsilon_1 + \varepsilon_2}{2} \\ S_B = E\dfrac{\varepsilon_1 - \varepsilon_2}{2} \end{cases} \quad (2)$$

where N is the axial force, M is the bending moment, A is the section area, R is the radius, and E is the Young modulus.

Each VWS sensor node consists of 4 channels by design; hence, one node for each section will satisfy the measurement requirement. The total number of VWSs is 206, and the total number of wireless nodes is 59. The VWS is deployed to measure the strain with an accuracy of 5 με within the range of ±1500 με and the temperature with an accuracy of 0.5℃ within the range of -10 to 60℃. In addition, 17 acceleration sensors are distributed on the pipe trusses and columns to measure the responses to the excitation of a passing train. Triaxial MEMS accelerometers are used for vibration measurement with the amplitude ranging from -8 to +8 g and a sensitivity of 64000 LSB/g.

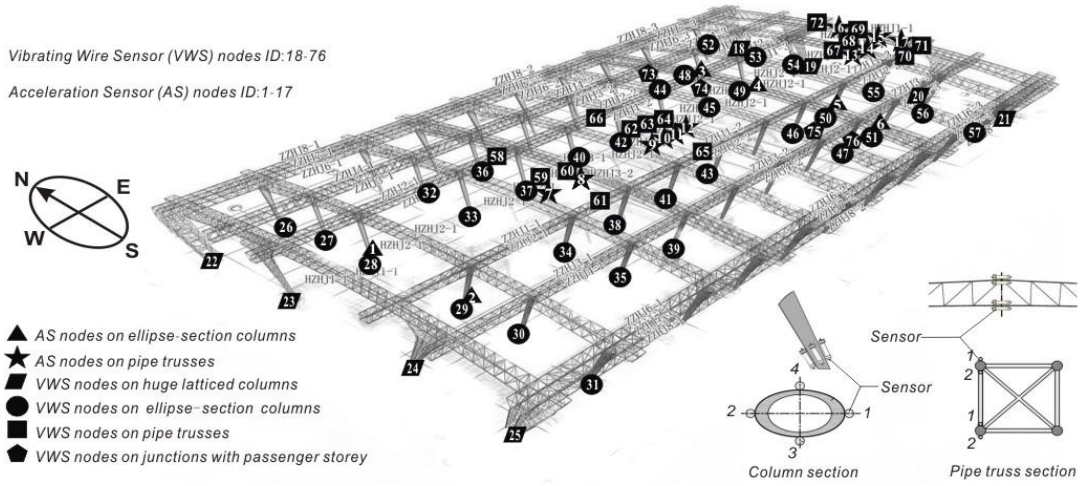

Fig. 9 Layout of all sensor nodes in the steel structure

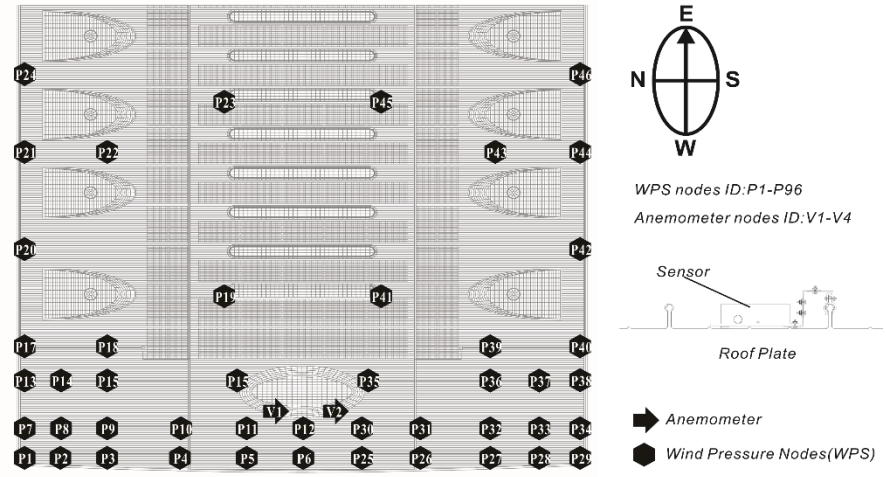

Fig. 10 Layout of all wind sensor nodes on the western half of the roof

Table 2 Distribution of the sensor nodes on the railway station

Sensor type	Acceleration		VWS and temperature				Wind pressure	Wind speed
Serial numbers	1 - 6	7 - 17	18 - 25	26 - 57	58 - 72	73 - 76	P1 - P96	V1 - V4
Total numbers	6	11	32	128	30	16	96	4
Location	Ellipse-section columns	Pipe trusses	Latticed columns	Ellipse-section columns	Pipe trusses	Story junctions	Roof sheathings	Roof sheathings

Table 3 Parameters of sensors

Sensor type	VWS	Temperature	Wind speed	Wind pressure	Acceleration
Range	±1500 με	-10~60℃	0~40 m/s	±2.5 kPa	±8 g
Accuracy	5 με	0.5°	0.1 m/s	0.076 Pa	64000 LSB/g

(a) VWS senor nodes (b) Wind speed and pressure sensor nodes

Fig. 11 Photos of sensor nodes installed on the site

To obtain the wind load distribution on the roof, a total of 96 wind pressure sensors and 4 wind speed sensors are installed. The sensors used in wind field monitoring measure the wind speed and pressure with a set measuring range (wind pressure: ±2.5 kPa, and wind speed: 0~40 m/s) and good accuracy (wind pressure: 0.076 Pa, and wind speed: 0.1 m/s). The layout of all sensor nodes is presented in Figs. 9-10, and total numbers and parameters of the sensors are listed in Tables 2-3. Photos of the typical sensor nodes installed on the site are shown in Fig. 11.

The network installation process has been influenced by many factors, such as the large architectural scope and the construction process. Therefore, a three-layer tree-type network is customized, and it continues to expand from both the east and west sides according to the construction process, as illustrated in Fig. 12. The whole data flow of the WSN that is customized for the railway station is clearly illustrated in the figure. An IPC that is connected online via a WLAN is used as an on-site server, and the data that are collected from all sensor nodes via the sink node are subsequently transmitted over the internet. Any client can acquire monitoring data from an on-site server by employing their access permission for the database.

3.3 Monitoring scheme and performance of the SHM system

The monitoring scheme is the foremost critical issue during the whole life cycle of the railway station. With optimized management of the data collection, the regular battery replacement cycle will last longer, which will minimize the loss of monitoring information, and improve the system's efficiency. The standardized operating mode is maintained for regular data collection during the life cycle. In this mode, the SHM system collects data from all sensors with short sampling time and low sampling rates, which

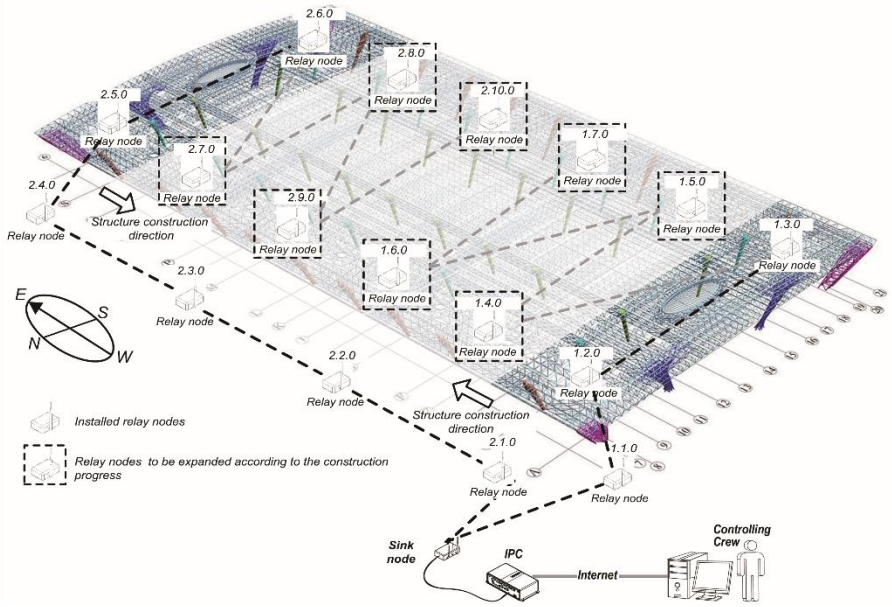

Fig. 12 Customized tree-type network for the railway station

Table 4 Specific information of the two working modes

Working mode	Sensor node	Sampling time cycle	Sampling time	Sampling rate
Standardized operating mode	VWS and temperature	Once per 8 hours	30 s	0.1 Hz
	Acceleration	Once per day	2 min	50 Hz
	Wind speed	Once per day	10 min	2 Hz
	Wind pressure	Once per day	2 min	20 Hz
Centralized collection mode	VWS and temperature	Depending on events	Consecutive collection	0.1 Hz
	Acceleration			50 Hz
	Wind speed			1 Hz
	Wind pressure			2 Hz

will reduce the battery consumption. The strain and temperature data from the VWS are collected 3 times a day because their fluctuations are quasi static. For the accelerator and wind field monitoring, the data are commonly related to specific events such as typhoons, earthquakes, or critical construction procedures, so the system can transfer the working mode to a centralized collection mode when those events are encountered. For strong wind events, the consecutive data collection of all sensors is activated remotely to capture the real-time status of structures according to meteorological forecasts. The specific information about these two modes of the monitoring system is listed in Table 4.

The rate of data losing (RDL) of all sensors is a critical indicator for evaluating the performance of the SHM system. For VWS sensor nodes, the daily RDL in the standardized operating mode has been recorded for 6 months after a regular battery replacement in April 2018. Each VWS sensor node consists of 4 channels as described in Section 3.2, and the daily RDL can be expressed as Eq. (3)

$$RDL = 1 - \frac{\sum_i^n N_i'}{\sum_i^n N_i} \quad (3)$$

where RDL is the daily RDL, N_i is the scheduled amount of data of the i_{th} channel, N_i' is actual amount of data of the i_{th} channel, and n is the number of channels. Due to the page limit of this paper, the RDLs of the selected sensor nodes are plotted in Fig. 13. The discontinuity in the data set from Aug. 5th, 2018 to Aug, 14th, 2018 is due to an accidental shutdown of the onsite server. It is found that the RDL was close to zero most of the time. Occasionally the communication between the relay nodes and sensor nodes fails due to signal obstruction in the complicated roof system, and the daily RDL is found to be less than 0.12.

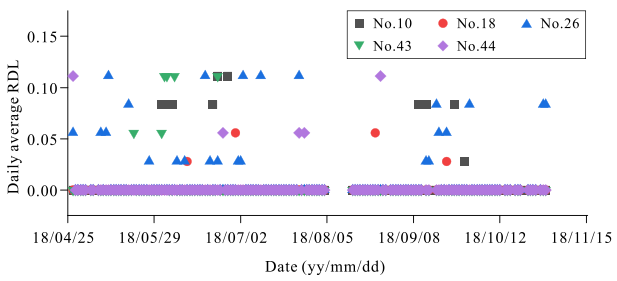

Fig. 13 Daily RDL

4. Analysis of the monitoring data during the life cycle

A total of 323 sensors, which collected data via the WSN during the construction stage (2009 - 2014) and the in-service stage (2014 - present), were installed on the entire structure. A large amount of data on the strain, temperature, acceleration, and wind load have been collected, and actual structural behaviors are revealed by the monitoring data, which validates the performance of the wireless SHM system, such as the system being reliable data transfer mechanism and convenient remote operating system. This section analyzes the monitoring data collected by various sensors, including the stress variations during the lifting processes of steel pipe trusses, the internal force retributions during by the entire construction processes, the vibrations are caused by the passing trains, the relationship between the strain and the temperature in long-term monitoring, and the wind load on the roof.

4.1 Stress tracking during the integral lifting of the steel pipe trusses

All steel pipe trusses of the roof system were divided into 29 units according to the axis position. Examples of lifting processes on the east side of the railway station are shown in Fig. 14. For each truss unit, eight steps can be defined in the lifting process:

(1) Assemble trusses on the ground;
(2) Increase the lifting force by 50%;
(3) Increase the lifting force by 100%, and lift the truss to 30 cm above the ground;
(4) Maintain the height to inspect the equipment;
(5) Start lifting;
(6) Lift the truss unit to the exact position;
(7) Assemble the other components for connecting the lifted truss with the entire assemble structure; and
(8) Remove the temporary support.

Finite element analysis (FEA) is carried out to simulate the lifting processes of the truss units. A commercial structural analysis software, Midas/Gen, is used for the model and analyses of the lifting processes. The truss unit shown in Fig. 14 is built by using 2084 beam elements with different sectional properties. Sensor validation is achieved by comparing the FEA results with the monitoring data. In

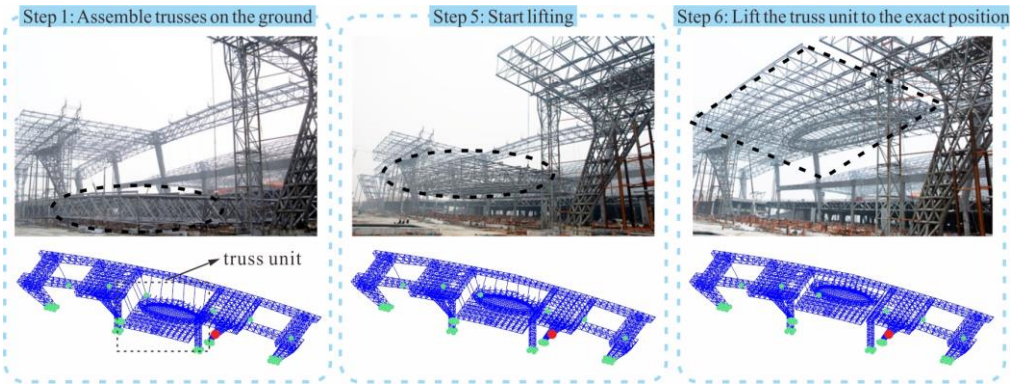

Fig. 14 Examples of integral truss lifting during the construction in area S-U/12-15

each lifting step, the strain variation at each sensor point was tracked. The bending stresses (S_B) and axial stresses (S_A) are calculated from two monitored symmetrical surface strains (ε_1 and ε_2) using Eq. (2). A truss unit located in Area S-U/12-15 is considered as an example. Area S-U/12-15 is bounded by axis-S, axis-U, axis-12, and axis-15, and the serial numbers of the axes are shown in Fig. 8. Areas are identified using the same method.

In different construction steps, the stresses of the structure are obtained via the FEA and compared with the measurements. The stress variation curves of the ellipse-shaped cross-section column during the lifting steps are plotted in Figs. 15(b)-(c), and a red mark shown in Fig. 15(a) represents the measurement position on the column. The relative deviations between the monitored data and the numerical results are found to be large in the first three steps due to the vibration of lifting jacks at the beginning of the lifting stage. The construction process remains stable and quasi-static as the truss unit rises, so the monitored stresses become reasonably close to the FEA results with a relative deviation in 2.4%~18.3%. The deviation is due to uncertain construction error, the difference between the FE model and the actual structure, and environmental effects such as a nonuniform temperature. However, all stress values are found to be within the allowable stress of the steel material.

4.2 Stress tracking throughout the construction process

For the entire structural construction process, the condition of each roof truss and column unit can be divided into four phases: the lifting of the truss, the lifting of the adjacent roof truss, the lifting of other roof trusses, and the installation of roof purlins. As an example, the variations of the stresses are briefly presented in Fig. 16, where Stresses 1 and 2 represent two symmetrical surface stresses. The deviations of Stresses 1 and 2 reflect the bending moment changes. The stresses on the ellipse-shaped cross-section column and the latticed column are relatively stable and increase with the construction process. The stresses on the upper and lower beams of the roof truss include both bending and axial stresses, and the largest stress is within 70.2 MPa, which is within the allowable stress of the steel

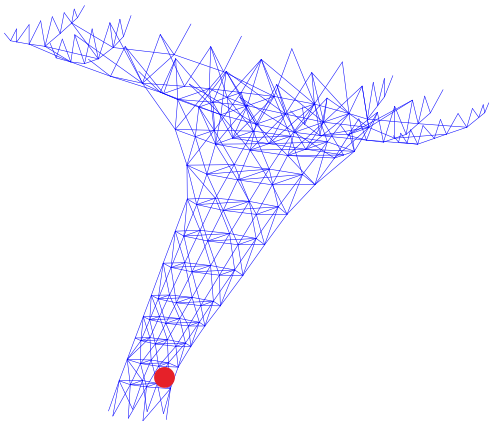

(a) FE model of an ellipse-shaped column

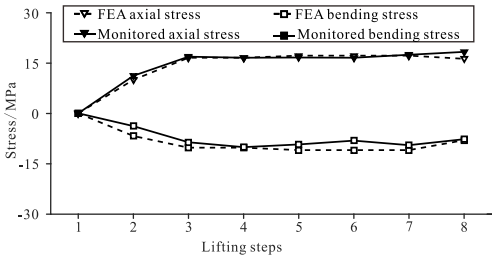

(b) Symmetrical surface stresses of an ellipse-shaped column

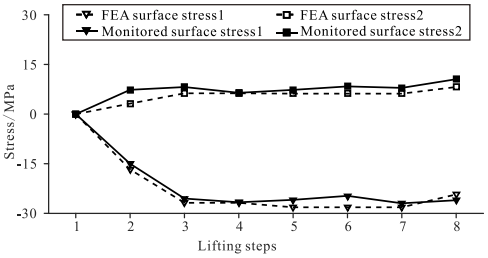

(c) Axial and bending stresses of an ellipse-shaped column

Fig. 15 Stress tracking during the integral lifting of a component located in Area S-U/12-15

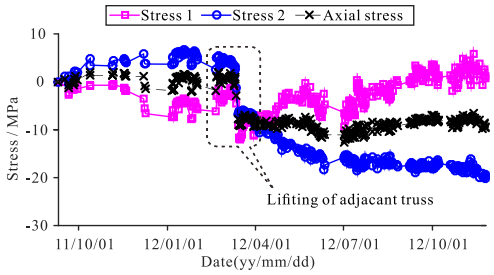

(a) An ellipse-shaped column located in Area C/20-21

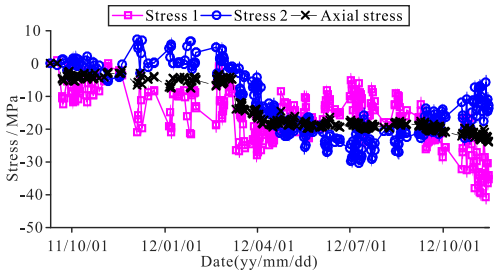

(b) A large lattice column located in Area A/15-12

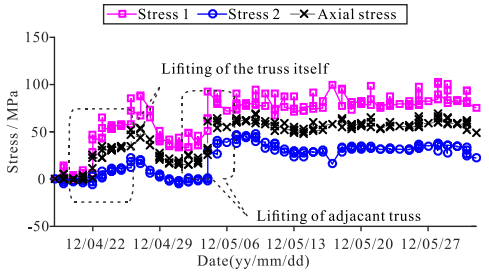

(c) An upper beam of pipe truss located in Area G-H/12-13

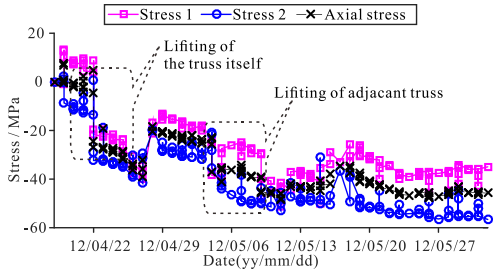

(d) A lower beam of pipe truss located in Area G-H/12-13

Fig. 16 Measured stress variations of typical components during the lifting process

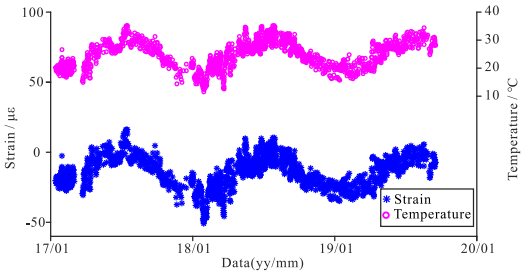

(a) The truss located in Area D11/12

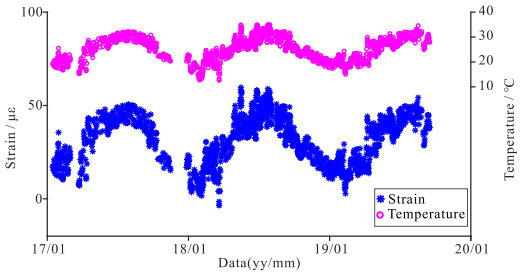

(b) The truss located in Area C15/16

Fig. 17 Variations of the strain and temperature over the last three years

material. The stress increments are substantial during the lifting processes of the truss and of the adjacent truss, and become relatively stable afterwards. Throughout the construction process, the stress variations of all monitored components do not differ substantially from the result of the theoretic analysis; Therefore, we conclude that the stress redistribution remains within the safe range.

4.3 Relationship between the strain and temperature in long-term monitoring

Data have been collected from over 300 sensors, including VWSs, accelerometers, and anemographs, since the beginning of construction. After the completion of the railway station, we focus on the long-term temperature-dependent structural behavior of the large-scale steel roof. Considering the roof trusses located in Area D11/12 and Area C15/16 as examples, the variations of the strains and temperature are plotted in Fig. 18. The correlation coefficients R^2 of the strain data and the temperature data in Fig. 18 are found to be 0.982 and 0.903 in the two areas, respectively, which indicates a strong linear relationship between the temperature and strains.

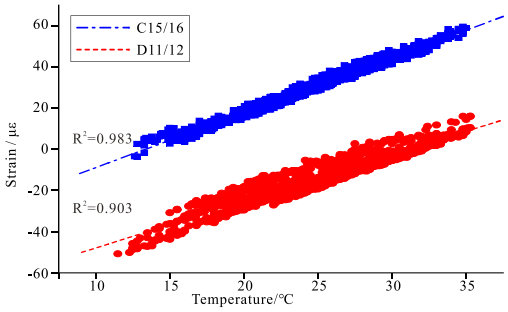

Fig. 18 Relationship between the temperature and the strain

4.4 Vibration caused by passing trains

A main common feature of the large-scale railway stations is “bridge-building combination”: trains always pass through, instead of passing by, the station. Therefore, the vibration that is caused by the train cannot be ignored. A total of 17 acceleration sensors were installed to monitor the vibration of the roof truss and columns. The column units located in Area Q/10-12 are considered as an example. Acceleration data were obtained in three directions over

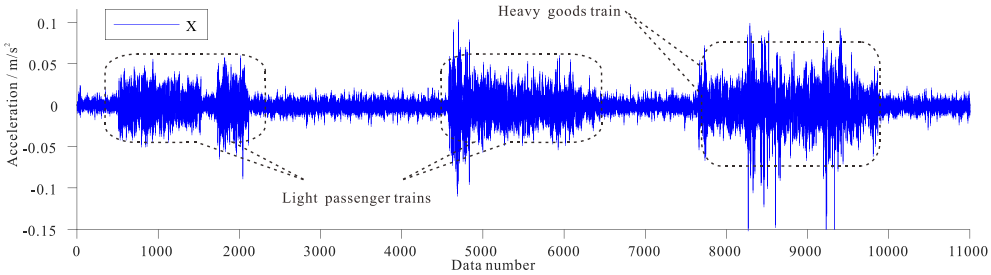

(a) X-direction acceleration on the column

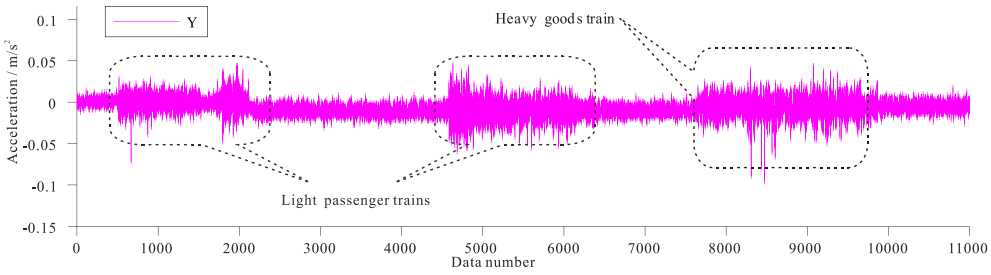

(b) Y-direction acceleration on the column

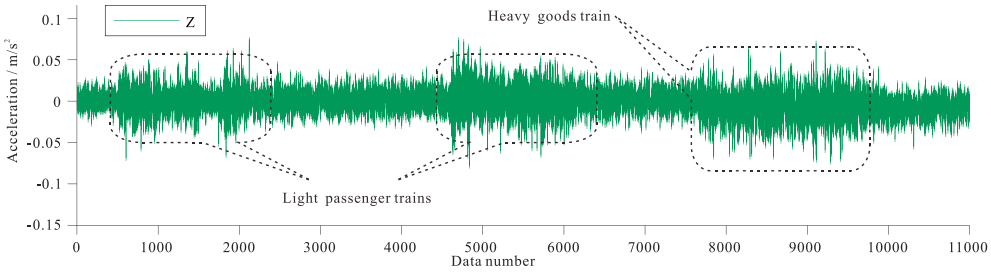

(c) Z-direction acceleration on the column

Fig. 19 Vibrations in Area Q/10-12 caused by three passing trains

approximately 15 minutes. During this period, two light passenger trains and a heavy freight train passed through the station. The acceleration curve of one node on the roof truss and columns is shown in Fig. 19. The vibration amplitude caused by the heavy freight train was found to be 1.5 times larger than those caused by the light passenger trains during the construction.

4.5 Wind load on the roof

The monitoring data on the wind velocities at V1 and V2 (Fig. 10) are plotted in Fig. 20, and they have a velocity range of 0.21~9.79 m/s. The wind velocities and the wind directions at the two locations are very close, and there are no abnormal values; hence, the wind velocity sensors and the wireless communication system are found to be highly stable. The wind load is one of the main loads for the large-span steel roof structures. Hence, long-term measurements of the wind load have been obtained on the roof. The dynamic wind pressures at various locations shall also be considered during the vibration analysis. If the wind velocity rapidly increases on the structure's surface, the wind pressure rapidly increases in the compression. Fig. 21 shows the time histories of the fluctuating components of the wind velocity (FWV) at V1 and the wind pressure at 5 nodes (from P8 to P12). The effect of the rapid change in

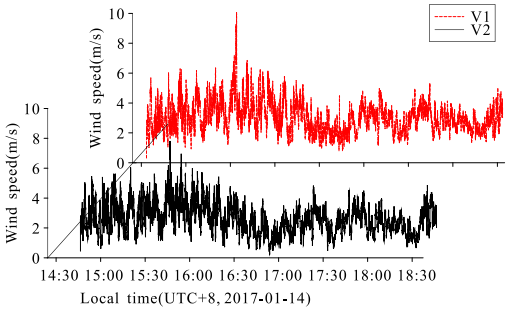

(a) Wind velocities at V1 and V2

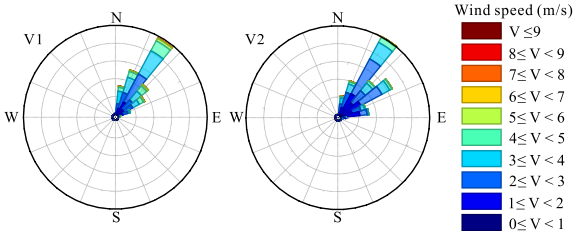

(b) Wind roses of V1 and V2

Fig. 20 Time histories of the wind velocities and direction

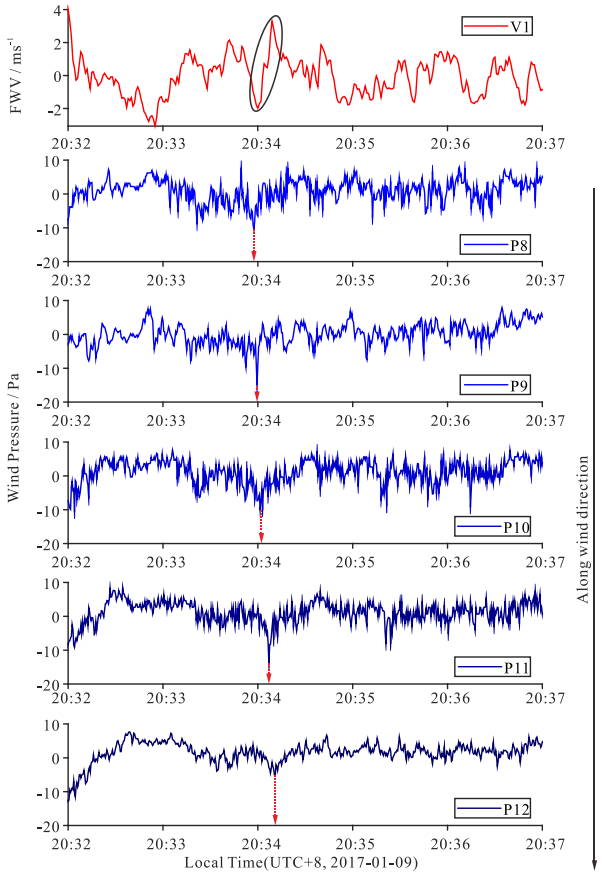

Fig. 21 Fluctuating wind pressures and velocities at various nodes along the direction of the wind

the wind velocity, as in the black ellipse marked in Fig. 21, did not occur at the same time among the wind pressure nodes. The red arrows in Fig. 21 show the peak wind pressures during this rapid increase of the wind velocity. A small delay is observed in the wind pressure time histories at the nodes (P10~P12) that are close to the wind-ward edge.

5. Conclusions

An SHM system using a customized WSN has been successfully deployed on the Hangzhou East Railway Station in China, and the results verify the performances of the monitoring equipment and the data transfer mechanism. The focus of this paper is the full-scale development of an SHM using a robust customized WSN for the whole life cycle of a railway station including the construction and in-service stages. The following conclusions can be drawn:

(1) Considering the effect of the construction process and the on-site environment, the customized WSN system uses four types of sensors as measurement components: a VWS for the strains, acceleration, temperature, and wind load. Each independent MTS module enables the multitype sensors to operate together in the network of Hangzhou East Railway Station. The daily rate of data losing in the standardized operating mode has been recorded for 6 months after a regular battery replacement in April 2018, and it is found that the RDL was close to zero most of the time. The wireless sensor nodes are proven to be stable and durable.

(2) The customized WSN is developed with an adjustable tree-type topology and a controllable operating mechanism for data and battery power management. The basic structure of the WSN is a tree-type network that realizes robust communication over the entire structure. Using the standardized monitoring scheme in Table 4, the regular battery replacement period of the WSN is longer than 6 months. The WSN is found to have the advantages of adjusting number of sensor nodes flexibly and extending the monitoring area without any limitation of the wireless transmission distance, which is satisfactory for meeting the requirements of many multitype sensors in large-span spatial structures.

(3) According to the data analysis results, the effects of the construction process and the on-site environment on the super-large-scale structure are found to be substantial. The stress increments on the roof trusses are large only during the lifting processes of the trusses, and they become relatively stable afterwards. The monitored stresses become reasonably close to the theoretical results with the relative deviation in 2.4%~18.3% during the lifting process. All the stress values are found to be within the allowable stress of the steel material. As a result, the SHM system ensured the construction precision and structural safety of Hangzhou East Railway Station including the construction stage.

(4) During the in-service stage, the steel structure is mainly subjected to the environmental loadings, such as wind loads and temperature loads. The correlation coefficients R^2 of the strain data and the temperature are found to be 0.982 and 0.903 at two typical locations, respectively, which indicates there is a strong linear relationship between the ambient temperature and strains of the roof trusses after the completion of the structure.

Acknowledgments

The work described in this paper was supported by the National Key R&D program of China (2017YFC0806100), National Natural Science Foundation of China (Grant No. 51578491 and No. 51178415), Qianjiang Scholar Foundation of Zhejiang province (2013R10038) and the Scientific Research Foundation for the Returned Overseas Chinese Scholars, State Ministry of Education.

References

Akyildiz, I.F., Su, W., Sankarasubramaniam, Y. and Cayirci, E. (2002), "Wireless sensor networks: a survey", *Comput. Netorks*, **38**(4), 393-422. https://doi.org/10.1016/S1389-1286(01)00302-4

Bennett, P.J., Soga, K., Wassell, I., Fidler, P., Abe, K., Kobayasni, Y. and Vanicek, M. (2010), "Wireless sensor networks for

underground railway applications: case studies in Prague and London", *Smart Struct. Syst., Int. J.*, **6**(5-6), 619-639. https://doi.org/10.12989/sss.2010.6.5_6.619

Chae, M.J., Yoo, H.S., Kim, J.Y. and Cho, M.Y. (2012). "Development of a wireless sensor network system for suspension bridge health monitoring", *Automat. Constr.*, **21**, 237-252. https://doi.org/10.1016/j.autcon.2011.06.008

Cho, S., Jo, H., Jang, S., Park, J., Jung, H.J., Yun, C.B., Spencer Jr, B.F. and Seo, J.W. (2010), "Structural health monitoring of a cable-stayed bridge using wireless smart sensor technology: data analyses", *Smart Struct. Syst., Int. J.*, **6**(5-6), 461-480. https://doi.org/10.12989/sss.2010.6.5_6.461

De Battista, N. (2013), "Wireless Technology and Data Analytics for Structural Health Monitoring of Civil Infrastructure", Doctoral Dissertation; University of Sheffield, UK.

Dong, X., Zhu, D., Wang, Y., Lynch, J.P. and Swartz, R.A. (2014), "Design and validation of acceleration measurement using the Martlet wireless sensing system", *Proceedings of ASME 2014 Conference on Smart Materials, Adaptive Structures and Intelligent Systems*, American Society of Mechanical Engineers Digital Collection.

He, X.H., Shi, K. and Wu, T. (2018), "An integrated structural health monitoring system for the Xijiang high-speed railway arch bridge", *Smart Struct. Syst., Int. J.*, **21**(5), 611-621. https://doi.org/10.12989/sss.2018.21.5.611

Hou, T.C., Lynch, J.P. and Parra-Montesinos, G. (2005), "In Situ Wireless Monitoring of Fiber Reinforced Cementitious Composite Bridge Piers", *Proceedings of the 23rd International Modal Analysis Conference*, Orlando, FL, USA, January.

Jang, S., Jo, H., Cho, S., Mechitov, K., Rice, J.A., Sim, S.H., Jung, H.J., Yun, C.B., Spencer Jr, B.F. and Agha, G. (2010), "Structural health monitoring of a cable-stayed bridge using smart sensor technology: deployment and evaluation", *Smart Struct. Syst., Int. J.*, **6**(5-6), 439-459. https://doi.org/10.12989/sss.2010.6.5_6.439

Jo, H., Sim, S.-H., Mechitov, K.A., Kim, R., Li, J., Moinzadeh, P., Spencer Jr., B.F., Park, J.W., Cho, S., Jung, H.-J., Yun, C.-B., Rice, J.A. and Nagayama, T. (2011), "Hybrid wireless smart sensor network for full-scale structural health monitoring of a cable-stayed bridge", In: *Sensors and Smart Structures Technologies for Civil, Mechanical, and Aerospace Systems*, International Society for Optics and Photonics, Vol. 7981, p. 798105.

Kane, M., Zhu, D., Hirose, M., Dong, X., Winter, B., Häckell, M. and Swartz, A. (2014), "Development of an extensible dual-core wireless sensing node for cyber-physical systems", In: *Sensors and Smart Structures Technologies for Civil, Mechanical, and Aerospace Systems 2014*, 9061, International Society for Optics and Photonics, p. 90611U.

Kim, S., Pakzad, S., Culler, D., Demmel, J., Fenves, G., Glaser, S. and Turon, M. (2007), "Health monitoring of civil infrastructures using wireless sensor networks", *Proceedings of the 6th International Conference on Information Processing in Sensor Networks*, pp. 254-263.

Lee, H.M., Kim, J.M., Sho, K. and Park, H.S. (2010), "A wireless vibrating wire sensor node for continuous structural health monitoring", *Smart Mater. Struct.*, **19**(5), 055004. https://doi.org/10.1088/0964-1726/19/5/055004

Luo, Y.Z., Yang, P.C., Shen, Y.B., Yu, F., Zhong, Z.N. and Hong, J. (2014), "Development of a dynamic sensing system for civil revolving structures and its field tests in a large revolving auditorium", *Smart Struct. Syst., Int. J.*, **13**(6), 993-1014. https://doi.org/10.12989/sss.2014.13.6.993

Lynch, J.P., Law, K.H., Kiremidjian, A.S., Kenny, T.W., Carryer, E. and Partridge, A. (2001), "The design of a wireless sensing unit for structural health monitoring", *Proceedings of the 3rd International Workshop on Structural Health Monitoring*, Stanford University, Stanford, CA, USA.

Maser, K., Egri, R., Lichtenstein, A. and Chase, S. (1996), "Development of a Wireless Global Bridge Evaluation and Monitoring System", In: *Structural Materials Technology: An NDT Conference*, CRC Press, p. 245.

Meyer, J., Bischoff, R., Feltrin, G. and Motavalli, M. (2010), "Wireless sensor networks for long-term structural health monitoring", *Smart Struct. Syst., Int. J.*, **6**(3), 263-275. https://doi.org/10.12989/sss.2010.6.3.263

Ni, Y.Q., Xia, Y., Liao, W.Y. and Ko, J.M. (2009), "Technology innovation in developing the structural health monitoring system for Guangzhou New TV Tower", *Struct. Control Health Monitor.*, **16**(1), 73-98. https://doi.org/10.1002/stc.303

Ni, Y.Q., Li, B., Lam, K.H., Zhu, D.P., Wang, Y., Lynch, J.P. and Law, K.H. (2011), "In-construction vibration monitoring of a supertall structure using a long-range wireless sensing system", *Smart Struct. Syst., Int. J.*, **7**(2), 83-102. https://doi.org/10.12989/sss.2011.7.2.083

Pakzad, S.N., Fenves, G.L., Kim, S. and Culler, D. (2008), "Design and implementation of scalable wireless sensor network for structural monitoring", *J. Infrastruct. Syst.*, **14**(1), 89-101. https://doi.org/10.1061/(ASCE)1076-0342(2008)14:1(89)

Park, J.H., Kim, J.T., Hong, D.S., Mascarenas, D. and Lynch, J.P. (2010), "Autonomous smart sensor nodes for global and local damage detection of prestressed concrete bridges based on accelerations and impedance measurements", *Smart Struct. Syst., Int. J.*, **6**(5-6), 711-730. https://doi.org/10.12989/sss.2010.6.5_6.711

Park, H., Lee, H., Choi, S. and Kim, Y. (2013), "A practical monitoring system for the structural safety of mega-trusses using wireless vibrating wire strain gauges", *Sensors*, **13**(12), 17346-17361. https://doi.org/10.3390/s131217346

Phanish, D., Garver, P. W., Matalkah, G., Landes, T., Shen, F., Dumond, J., Abler, R., Zhu, D., Dong X., Wang Y. and Coyle, E. J. (2015), "A wireless sensor network for monitoring the structural health of a football stadium", *Proceedings of 2015 IEEE 2nd World Forum on Internet of Things* (*WF-IoT*), pp. 471-477. https://doi.org/10.1109/WF-IoT.2015.7389100

Qu, W., Teng, J., Xiang, H., Zhong, L., Liu, H., Wang, J. and Li, G. (2006), "Intelligent health monitoring for roof space truss structure of the Shenzhen Citizen Center under wind load", *Jianzhu Jiegou Xuebao* (*Journal of Building Structures*), **27**(1), 1-8.

Rice, J.A., Mechitov, K., Sim, S.H., Nagayama, T., Jang, S., Kim, R. and Fujino, Y. (2010), "Flexible smart sensor framework for autonomous structural health monitoring", *Smart Struct. Syst., Int. J.*, **6**(5-6), 423-438. https://doi.org/10.12989/sss.2010.6.5_6.423

Ruiz-Sandoval, M.E., Spencer Jr., B.F. and Kurata, N. (2003), "Development of a high-sensitivity accelerometer for the Mica platform", *Proceedings of the 4th International Workshop on Structural Health Monitoring*, Stanford, CA, USA.

Spencer Jr, B.F. and Cho, S. (2011), "Wireless smart sensor technology for monitoring civil infrastructure: technological developments and full-scale applications", *Proceedings of the World Congress on Advances in Structural Engineering and Mechanics* (*ASEM'11*), Seoul, Korea, September, pp. 1-28.

Stajano, F., Hoult, N.A., Wassell, I.J., Bennett, P.J., Middleton, C.R. and Soga, K. (2010), "Smart bridges, smart tunnels: Transforming wireless sensor networks from research prototypes into robust engineering infrastructure", *Ad Hoc Networks*, **8**(8), 872-888. https://doi.org/10.1016/j.adhoc.2010.04.002

Straser, E.G. and Kiremidjian, A.S. (1996), "A modular visual approach to damage monitoring for civil structures", *Proceedings of SPIE v2719, Smart Structures and Materials*, Vol. 96, pp. 112-122.

Straser, E.G., Kiremidjian, A.S. and Meng, T.H. (2001), "Modular wireless damage monitoring system for structures e.g. for earthquakes, has several modular, battery powered data acquisition devices which transmit structural information to central data collection", U.S. Patent; No. 6,292,108. Washington, DC, USA.

Sun, X., Wand, Q., Zhu, M. and Wu, M.C. (2015), "Application of optical fiber Bragg grating strain gauge to cable force monitoring of FAST", *Optics Precision Eng*., **23**(4), 919-925.

Swartz, R.A., Lynch, J.P., Zerbst, S., Sweetman, B. and Rolfes, R. (2010), "Structural monitoring of wind turbines using wireless sensor networks", *Smart Struct*. *Syst*., *Int*. *J*., **6**(3), 183-196. https://doi.org/10.12989/sss.2010.6.3.183

Teng, J., Zhu, Y.H., Lu, W. and Xiao, Y.Q. (2010), "The intelligent method and implementation of health monitoring system for large span structures", In: *Earth and Space 2010: Engineering*, *Science*, *Construction*, *and Operations in Challenging Environments*, pp. 2543-2552.

Townsend, C.P. and Arms, S.W. (2005), "Wireless sensor networks: Principles and applications", In: (J. Wilson, ed.) *Sensor Technology Handbook* - Chapter 22. Elsevier, pp. 575-589.

Ye, W., Heidemann, J. and Estrin, D. (2002), "An energy-efficient MAC protocol for wireless sensor networks", *Proceedings of the 21st Annual Joint Conference of the IEEE Computer and Communications Societies*, Vol. 3, pp. 1567-1576.

Yi, T.H., Li, H.N. and Zhang, X.D. (2015), "Health monitoring sensor placement optimization for Canton Tower using immune monkey algorithm", *Struct*. *Control Health Monitor*., **22**(1), 123-138. https://doi.org/10.1002/stc.1664

Yi, Z., Kim, C.W., Tee, K.F., Garg, A. and Garg, A. (2018), "Long-term health monitoring for deteriorated bridge structures based on copula theory", *Smart Struct*. *Syst*., *Int*. *J*., **21**(2), 171-185. https://doi.org/10.12989/sss.2018.21.2.171

Zhang, Z. and Luo, Y. (2017), "Restoring method for missing data of spatial structural stress monitoring based on correlation", *Mech*. *Syst*. *Signal Process*., **91**, 266-277. https://doi.org/10.1016/j.ymssp.2017.01.018

Zonta, D., Wu, H., Pozzi, M., Zanon, P., Ceriotti, M., Mottola, L., Picco, G.P., Murphy, A.L., Guna, S. and Corra', M. (2010), "Wireless sensor networks for permanent health monitoring of historic buildings", *Smart Struct*. *Syst*., *Int*. *J*., **6**(5-6), 595-618. https://doi.org/10.12989/sss.2010.6.5_6.595

Zou, Z., Nagayama, T. and Fujino, Y. (2014), "Efficient multihop communication for static wireless sensor networks in the application to civil infrastructure monitoring", *Struct*. *Control Health Monitor*., **21**(4), 603-619. https://doi.org/10.1002/stc.1588

HJ